Research Square

Preprints are preliminary reports that have not undergone peer review.
They should not be considered conclusive, used to inform clinical practice,
or referenced by the media as validated information.

Monitoring Cocoa Health and Productivity Using Multispectral and Thermal Remote Sensing: A Thirty-Year Longitudinal Study in Sunyani West Municipality, Ghana

PRINCE KWAKU MENSAH

princekwakumensah2@gmail.com

University of Energy and Natural Resources

ADIZAH MORRO

University of Energy and Natural Resources

HENRY TEI APOCHIE

University of Energy and Natural Resources

Research Article

Keywords: cocoa monitoring, remote sensing, NDVI, land surface temperature, land-use change, Ghana, Sunyani West, smallholder agriculture

Posted Date: April 27th, 2026

DOI: https://doi.org/10.21203/rs.3.rs-9515877/v1

License: This work is licensed under a Creative Commons Attribution 4.0 International License.
Read Full License

Additional Declarations: No competing interests reported.

Abstract

Cocoa (Theobroma cacao L.) production in Ghana faces mounting threats from climate variability, land-use change, and intensifying thermal stress. Yet spatially explicit, long-term assessments of cocoa health using remote sensing remain scarce for peri-urban districts of the Ghanaian cocoa belt. This study employs a 30-year longitudinal remote sensing analysis (1994–2024) over the Sunyani West Municipality, Bono Region, Ghana, integrating Landsat 5, 7, and 9 multispectral and thermal imagery to: (i) map cocoa-growing areas using Support Vector Machine (SVM) classification; (ii) assess temporal changes in cocoa vegetation health through the Normalized Difference Vegetation Index (NDVI); and (iii) quantify the relationship between land surface temperature (LST) variation and cocoa crop performance. Results reveal a significant spatial contraction of closed-forest cover from 26,937 ha (1994) to 9,046 ha (2024) alongside an 89% expansion of built-up and bareland areas, driven by rapid urbanization. Mean NDVI in cocoa zones declined progressively from 0.72 (1994) to 0.53 (2024), coinciding with a six-fold expansion of areas experiencing temperatures exceeding 37°C from 2.37% of the municipality in 1994 to 15.88% in 2024. Cocoa yields recorded minimum values of 0.55–0.60 tons ha^{-1} in years of peak thermal anomaly. A significant inverse relationship between LST and NDVI was identified, indicating that landscape-scale thermal stress, amplified by deforestation and urban heat-island effects, is a principal driver of declining cocoa health. These findings underscore the urgent need for integrated land-use planning, agroforestry expansion, and spatially targeted extension services in cocoa-producing peri-urban districts of West Africa.

1. Introduction

Cocoa (Theobroma cacao L.) is a cornerstone of Ghana's agricultural economy, contributing substantially to national export revenues and sustaining the livelihoods of approximately 800,000 smallholder farming households (Wessel & Quist-Wessel, 2015). Ghana ranks as the world's second-largest cocoa producer, with annual output exceeding 800,000 metric tons and accounting for nearly 20% of global supply (International Cocoa Organization, 2021). The Sunyani West Municipality in the Bono Region constitutes one of the country's principal cocoa-growing zones, where cultivation underpins the rural economy and community welfare (Asante et al., 2017). However, cocoa production in this district faces escalating pressures from climate variability, pest and disease incidence, ageing plantations, and soil fertility decline all of which threaten crop health and productivity (Abdulai et al., 2018).

Conventional monitoring of cocoa plantation health relies predominantly on visual field assessments, which are labour-intensive, spatially limited, and often too delayed to detect early-onset stress before significant yield loss occurs (Ruf et al., 2015; Babin et al., 2010). Given that smallholder cocoa farms in Ghana typically range between 1 and 3 hectares (Asare et al., 2017), systematic landscape-scale monitoring through ground surveys is logistically impractical and economically prohibitive. The imperative for scalable, cost-effective monitoring tools has intensified as cocoa-growing regions confront accelerating environmental pressures.

Remote sensing offers a transformative solution to these monitoring challenges. Multispectral satellite imagery enables the assessment of vegetation condition across extensive landscapes through spectral indices such as the Normalized Difference Vegetation Index (NDVI), which correlates strongly with leaf area index and chlorophyll content (Rouse et al., 1974; Tucker, 1979; Xue & Su, 2017). Thermal infrared imagery complements these optical measures by quantifying land surface temperature (LST) a proxy for canopy thermal stress and evapotranspiration deficit that often manifests physiologically before visible foliar symptoms appear (Jones et al., 2009; Maes & Steppe, 2019). The integration of multispectral and thermal sensing therefore provides a more holistic characterisation of cocoa health than either modality alone.

Despite the well-documented efficacy of remote sensing for agricultural monitoring, its application to cocoa health assessment in West Africa remains comparatively limited. Most existing studies have focused on land-use classification and deforestation detection rather than crop-condition monitoring (Koranteng et al., 2020; Kalischek et al., 2022; 2023). The complex canopy architecture of cocoa agroforestry systems characterised by multi-species composition, variable shade densities, and spectral similarity to adjacent forest cover presents distinct interpretive challenges (Vaast & Somarriba, 2014). Furthermore, persistent cloud cover in humid tropical environments reduces the frequency of cloud-free optical observations (Asner, 2001), while the prevalence of smallholder farm parcels smaller than a Landsat pixel introduces mixed-pixel contamination (Kalischek et al., 2023).

This study addresses these knowledge gaps by conducting a 30-year longitudinal analysis (1994–2024) of cocoa land use, vegetation health, and thermal stress dynamics in the Sunyani West Municipality. Three specific objectives are pursued: (1) to map the spatial distribution of cocoa farms using Support Vector Machine (SVM) classification of multi-temporal Landsat imagery; (2) to assess temporal trends in cocoa vegetation health using NDVI; and (3) to quantify the influence of LST variation on cocoa crop health and productivity. By developing spatially explicit evidence at the district scale, this research aims to inform precision extension services, agroforestry-based adaptation strategies, and land-use planning frameworks relevant to cocoa-producing peri-urban districts across West Africa.

2. Study Area

The Sunyani West Municipality is located in the Bono Region of Ghana, encompassing approximately 1,165 km² between latitudes 7°20'–7°55'N and longitudes 2°20'–2°45'W (Fig. 1). The municipality borders the Wenchi Municipal to the north, Tano North District to the east, Sunyani Municipality to the south, and Dormaa East District to the west. The gently undulating topography, dissected by seasonal watercourses, creates heterogeneous microclimatic conditions suitable for cocoa cultivation. A network of all-weather roads connects the district to major commodity markets in Sunyani and beyond, facilitating agricultural trade.

The climate is humid tropical with a bimodal rainfall pattern: a primary wet season from April to July and a secondary wet season from September to November. Mean annual rainfall ranges between 1,200 and

1,800 mm, broadly adequate for cocoa cultivation, but recent decades have seen increasing interannual variability and shortened rainy seasons (Asante & Amuakwa-Mensah, 2015). Mean annual temperatures range from 24 to 29°C, with dry-season maxima occasionally exceeding 30°C beyond the upper thermal tolerance threshold for optimal cocoa physiology (Schroth et al., 2016). Soils are predominantly Ferric Acrisols, characterised by moderate-to-high fertility and well-drained structure. Cocoa farming concentrates in the eastern sub-districts, notably the Chiraa community, while the central zone is dominated by the regional administrative capital and the northern fringe by forest reserves.

3. Materials and Methods

3.1 Data Sources

This study employed freely accessible Landsat satellite imagery and secondary administrative and yield data. Table 1 summarises the materials used.

Table 1. Data sources used in the study

Material	Source
Landsat 5, 7 and 9 Imagery	USGS Earth Explorer
Cocoa Yield Data	Quality Control Division, COCOBOD
Cocoa Farm Shapefile	CHED, Ghana Cocoa Board
District Administrative Shapefile	Lands Commission of Ghana, SMD

Landsat 5 TM, Landsat 7 ETM+, and Landsat 9 OLI-2/TIRS-2 imagery was acquired via the USGS Earth Explorer portal. Images were selected for four temporal epochs 1994, 2004, 2014, and 2024 with cloud cover below 10% and acquisition timing in the primary dry season to minimise atmospheric interference and ensure within-epoch phenological consistency. Cocoa yield records (tons ha^{-1}) for the period 1994–2024 were obtained from the Quality Control Division of COCOBOD. Administrative and farm boundary shapefiles were sourced from the Lands Commission of Ghana and COCOBOD's CHED department. All spatial analyses were conducted in Esri ArcGIS 10.8; statistical computations were performed in Microsoft Excel.

3.2 Research Design

The study employs a quantitative, longitudinal earth-observation design, analysing four temporal cross-sections over a 30-year period. This approach enables detection of decadal-scale trajectories in land-cover change, vegetation health, and thermal stress that shorter-term studies cannot reveal. The methodology workflow is illustrated in Fig. 2.

3.3 Image Pre-processing

All Landsat scenes underwent a standardised pre-processing workflow to ensure radiometric and geometric consistency across epochs. Atmospheric correction was performed using the Dark Object Subtraction (DOS) method, which removes additive path radiance by assuming the darkest pixel has near-zero surface reflectance (Chavez, 1988). Cloud and cloud-shadow masking was applied using the Fmask algorithm, which leverages spectral and thermal thresholds to identify contaminated pixels (Zhu & Woodcock, 2012). Scanline-corrector failure artefacts in Landsat 7 ETM+ imagery was addressed through focal statistics-based gap-filling interpolation in ArcGIS. All images were co-registered to WGS 1984 / UTM Zone 30N to ensure positional consistency across epochs.

3.4 Land Use/Land Cover Classification

3.4.1 Support Vector Machine Classification

LULC classification was performed using a Support Vector Machine (SVM) supervised classifier with a Radial Basis Function (RBF) kernel, demonstrated to outperform conventional maximum likelihood classifiers in heterogeneous tropical agricultural landscapes (Forkuor et al., 2022; Kalischek et al., 2023). SVM parameters were optimised through grid search: penalty parameter C = 100, gamma tuned between 0.01 and 0.10 per epoch. Four LULC classes were delineated: closed forest, open forest, cocoa farm, and bare land/built-up area. Training samples were generated from high-resolution Google Earth historical imagery and digitised reference polygons, with a minimum of 80 training polygons per class per epoch.

3.4.2 Accuracy Assessment

Classification accuracy was evaluated following Congalton and Green (2019) using stratified random sampling, with a minimum of 50 validation points per class per epoch. Error matrices were computed for each epoch, yielding Producer's Accuracy (PA), User's Accuracy (UA), Overall Accuracy (OA), and the Kappa coefficient (κ). Results are presented in Table 2.

Table 2. Classification accuracy assessment across four temporal epochs (1994–2024)

Land Cover Class	1994 PA (%)	1994 UA (%)	2004 PA (%)	2004 UA (%)	2014 PA (%)	2014 UA (%)	2024 PA (%)	2024 UA (%)
Closed Forest	90.38	94.00	89.80	88.00	84.00	84.00	81.63	80.00
Open Forest	81.13	86.00	84.91	90.00	76.00	76.00	73.58	78.00
Bare Land/Built-up	90.20	92.00	87.76	86.00	80.00	88.00	75.00	90.00
Cocoa Farm	93.18	82.00	83.67	82.00	86.67	78.00	89.47	68.00
Overall Accuracy (%)	**88.50**	—	**86.40**	—	**81.30**	—	**79.00**	—
Kappa Coefficient (κ)	**0.847**	—	**0.820**	—	**0.753**	—	**0.720**	—

Note: PA = Producer's Accuracy; UA = User's Accuracy. All Overall Accuracy and Kappa values are statistically significant ($p < 0.001$).

3.5 Derivation of Land Surface Temperature (LST)

LST was retrieved from the thermal infrared bands of each Landsat sensor following the USGS–NASA standard retrieval algorithm. The procedure comprised four sequential steps:

Step 1 Digital number (DN) to spectral radiance conversion: For Landsat 5/7, the transformation L_λ = Gain × DN + Bias was applied using sensor-specific gain and bias values from image metadata. For Landsat 8/9, the equivalent radiance scaling equation $L_\lambda = M_L \times DN + A_L$ was used, where M_L and A_L are the radiance multiplicative and additive scaling factors respectively.

Step 2 Radiance to brightness temperature (BT): $BT = K_2 / \ln(K_1/L_\lambda + 1) - 273.15$ (°C), where K_1 and K_2 are the band-specific thermal calibration constants provided in Landsat metadata.

Step 3 Land surface emissivity (LSE) estimation: Emissivity was derived using the NDVI Thresholds Method (Sobrino et al., 2004), with emissivity set to 0.979 for pixels with NDVI > 0.5 (dense vegetation), 0.966 for bare surfaces (NDVI < 0.2), and proportional vegetation fraction-weighted values for transitional pixels.

Step 4 LST computation: $LST = BT / [1 + (\lambda \times BT / \rho) \times \ln(\varepsilon)]$, where λ is the effective wavelength of the thermal band (10.8 μm for Landsat 5/7/8/9), $\rho = h \times c/\sigma$ (1.438×10^{-2} m·K), and ε is the derived surface emissivity. This method yields physically meaningful, surface-emissivity-corrected temperature estimates appropriate for thermal stress analysis in cocoa agroforests.

3.6 Vegetation Index Calculation

The Normalized Difference Vegetation Index (NDVI) was calculated for each epoch from atmospherically corrected surface reflectance imagery:

NDVI = (NIR − Red) / (NIR + Red)

where NIR corresponds to Landsat Band 4 (Landsat 5/7) or Band 5 (Landsat 8/9), and Red corresponds to Band 3 (Landsat 5/7) or Band 4 (Landsat 8/9). NDVI values range from −1 to +1, with values above 0.4 typically indicative of healthy vegetation canopy. Temporal composites were generated by median-stacking cloud-free imagery within each epoch year to minimise residual atmospheric and phenological noise. NDVI statistics (mean, minimum, maximum, and standard deviation) were extracted specifically within the classified cocoa farm boundaries for each epoch to isolate crop-specific vegetation dynamics from surrounding land covers.

Whilst recognising NDVI's known saturation behaviour in high-biomass tropical canopies (Guthmann et al., 2021), the index was selected for its 30-year continuous archive availability, its demonstrated utility in long-term vegetation trend analysis, and its established application in cocoa monitoring studies in Ghana (Acheampong et al., 2021). Results are interpreted as relative trend indicators rather than absolute health classifiers, a methodological caveat explicitly recognised throughout the analysis.

3.7 Statistical Analysis

Descriptive statistics (mean, range, and coefficient of variation) were computed for NDVI and LST values within cocoa zones at each epoch. Temporal trends in NDVI, LST, and LULC area were assessed using decadal change magnitudes. The relationship between mean NDVI and mean LST in cocoa zones was examined through bivariate correlation analysis, with cocoa yield data used as an independent indicator of productivity. Statistical analyses were conducted in Microsoft Excel, with significance thresholds set at $\alpha = 0.05$. Spatial pattern analysis of NDVI and LST distributions was conducted using zonal statistics in ArcGIS.

4. Results

4.1 Land Use and Land Cover Change (1994–2024)

SVM classification revealed substantial LULC transformations over the 30-year study period (Fig. 3). Closed-forest cover contracted sharply from 26,937 ha in 1994 to 9,046 ha in 2024 a loss of approximately 66%, equivalent to 17,891 ha. Open-forest cover expanded considerably between 1994 and 2004 (reaching 58,152 ha), reflecting conversion of closed forest to secondary vegetation, before declining to 32,837 ha by 2024. Bare land and built-up areas demonstrated the most dramatic absolute growth, expanding 89% from 31,526 ha (1994) to 62,266 ha (2024). Cocoa farm areas concentrated in the eastern sub-districts, with 19,018 ha of former farmland converted to non-agricultural uses between 1994 and 2024.

Table 3: LULC Statistics

	Closed forest	Open forest	Bare land/Built-up	Cocoa farm
Area (ha) 1994	**26937**	**43085**	**31526**	**4307**
Area (%)	25.45	40.70	29.78	4.07
Area (ha) 2004	**22988**	**58152**	**17102**	**7615**
Area (%)	21.72	54.93	16.16	7.19
Area (ha) 2014	**25646**	**28408**	**43427**	**8376**
Area (%)	24.23	26.84	41.02	7.91
Area (ha) 2024	**9046.17**	**32836.59**	**62266.41**	**1707.48**
Area (%)	8.55	31.02	58.82	1.61
1994-2004	-3950	15067	-14424	3308
1994-2014	-1291	-14677	11900	4069
1994-2024	-17891	-10249	30740	-2600
Total	**-23132.25**	**-9859.41**	**28216.08**	**4776.03**

Conversion matrix analysis revealed that the dominant transition during 1994–2004 was from closed forest to open forest (95,079 ha), indicating forest degradation as the primary driver. By the third period (1994–2024), however, the landscape dynamics had fundamentally shifted, with massive conversions from all vegetated classes to bare land and built-up area dominating the transition matrices a temporal shift carrying important policy implications for land-use governance.

4.2 Vegetation Health of Cocoa Farms

Temporal NDVI analysis within classified cocoa farm boundaries revealed a progressive decline in vegetation health across the study period (Table 3; Fig. 4). Mean NDVI within cocoa zones fell from 0.72 in 1994 to 0.65 in 2004, 0.59 in 2014, and 0.53 in 2024 a cumulative decline of 0.19 NDVI units over three decades, indicating a sustained deterioration in photosynthetic activity and canopy vigour.

Table 3. Temporal trends in NDVI, LST, cocoa yield, and rainfall conditions (1994–2024)

Year	Mean NDVI (Cocoa Zones)	High-Temp Zone >37°C (%)	Cocoa Yield (tons/ha)	Rainfall Category
1994	0.72	2.37	0.85	Adequate
2004	0.65	7.40	0.60	Below average
2014	0.59	11.20	0.55	Erratic/reduced
2024	0.53	15.88	N/A*	Variable

Note: *2024 cocoa yield data not yet available at time of analysis. Rainfall categories based on reported farmer perceptions and district records.

Spatial analysis identified distinct intra-district heterogeneity. High NDVI values (> 0.6) concentrated in eastern and northern fringes characterised by higher shade tree density and proximity to forest margins, whereas low NDVI values (< 0.35) were predominantly observed in peri-urban transition zones around Sunyani town. This spatial patterning indicates that proximity to urbanisation and associated deforestation are significant modifiers of cocoa vegetation health at the landscape scale.

4.3 Land Surface Temperature Variation and Cocoa Health

LST retrieval revealed a pronounced warming trend across the municipality over the study period (Fig. 5). The proportion of the municipality experiencing LST exceeding 37°C expanded from 2.37% in 1994 to 7.40% in 2004, 11.20% in 2014, and 15.88% in 2024 a six-fold increase over three decades (Table 3). LST was highest in bare land and built-up surfaces, which exhibited temperatures 4–8°C above adjacent vegetated areas, demonstrating a clearly observable urban heat island effect. Dense cocoa-agroforest canopies maintained mean LST values 3–5°C below the municipal mean in corresponding epochs.

An inverse relationship between LST and NDVI within cocoa farm boundaries was consistently observed across all epochs. In years of greatest thermal anomaly (2004 and 2014), NDVI values recorded their lowest levels (0.65 and 0.59, respectively), coinciding with the lowest cocoa yield observations (0.60 and 0.55 tons ha^{-1}). Conversely, the 1994 epoch recorded the highest mean NDVI (0.72) and most productive cocoa yield (0.85 tons ha^{-1}). Spatial overlay confirmed that the highest thermal stress concentrations in 2014 and 2024 occurred in cocoa zones immediately adjacent to the expanding peri-urban built-up areas.

5. Discussion

5.1 Urbanisation, Deforestation, and Cocoa Land Loss

The 89% expansion of built-up and bareland areas documented in this study is consistent with broader patterns of peri-urban agricultural land loss reported across sub-Saharan Africa (Kabila et al., 2021;

Osumanu et al., 2020) and reflects the specific trajectory of urbanisation in Ghana's regional capitals. The conversion of 19,018 ha of former cocoa farmland to non-agricultural uses between 1994 and 2024 is not merely a local land-management concern but constitutes a structural threat to the economic base of the Bono Region. Comparable trajectories have been observed in peri-urban areas of Kumasi, where prime agricultural land surrounding the city has been progressively absorbed by urban expansion (Bempah et al., 2023).

A critical finding of the LULC transition analysis is the temporal shift in conversion drivers: during 1994–2004, agricultural expansion dominated, with large closed-forest areas converted to cocoa farms; by 2014–2024, urbanisation had entirely supplanted agricultural expansion as the primary landscape driver. This shift carries important policy implications. Land-use governance frameworks designed for an earlier era of agricultural-frontier expansion are ill-suited to managing contemporary peri-urban encroachment. Research has highlighted that many district spatial development plans in Ghana do not designate or protect agricultural land (Bempah et al., 2023), a gap that likely contributed to the unregulated cocoa farm conversion observed. Additionally, displaced cocoa farmers may drive indirect deforestation at new agricultural frontiers (Renier et al., 2025), a cascading effect that comprehensive landscape monitoring must account for.

5.2 NDVI as a Long-Term Indicator of Cocoa Vegetation Health

The progressive decline in mean NDVI from 0.72 to 0.53 within cocoa farm boundaries over 30 years represents a biophysically significant indicator of deteriorating canopy condition. This trajectory aligns with findings from analogous monitoring studies in Ghana (Acheampong et al., 2021) and corroborates farmer-reported observations of increasing tree dieback, disease incidence, and yield decline (Ofori et al., 2022; Agyei et al., 2023). The spatial heterogeneity of NDVI with high-performance zones in shaded, forest-proximate areas and stressed zones in peri-urban and deforested areas provides spatially actionable evidence for precision agricultural extension. Zones of moderate NDVI represent priority intervention areas, where targeted management improvements are most likely to yield production gains.

The known limitations of NDVI in high-biomass tropical systems particularly canopy saturation at moderate-to-high leaf area index values (Guthmann et al., 2021) were acknowledged in this study's design. NDVI was selected as a long-term trend indicator for its unique 30-year archival depth rather than as an instantaneous health classifier. Future monitoring protocols should incorporate Sentinel-2 red-edge indices, demonstrated by Moraiti et al. (2024) to substantially outperform NDVI for distinguishing cocoa canopy stress, alongside Sentinel-1 SAR backscatter to improve class separability and reduce cloud-cover sensitivity (Kalischek et al., 2022; 2023).

5.3 Land Surface Temperature and Cocoa Productivity

The six-fold expansion of areas exceeding 37°C between 1994 and 2024 constitutes a thermal stress trajectory of direct agronomic relevance. Cocoa physiology is adversely affected above 32°C, with heat stress reducing flower viability, pollination rates, and pod-set efficiency (Läderach et al., 2013; Anim-Kwapong & Frimpong, 2005). The concurrent observation that the highest-yield year (1994, 0.85 tons ha^{-1}) coincided with the lowest high-temperature zone extent (2.37%), and the lowest-yield years (2004 and 2014) with the greatest thermal anomalies, provides landscape-scale empirical support for the temperature-yield relationship documented in controlled studies.

The urban heat island signal where built-up surfaces were 4–8°C warmer than adjacent vegetated areas represents a locally amplified thermal stress mechanism potentially exacerbating regional climate warming beyond large-scale model projections (Asante et al., 2025). Shade tree management emerges as a critical thermal adaptation lever, with vegetated zones maintaining consistently lower LST. Given an estimated two million hectares of Ghana's cocoa land under low- or no-shade conditions (UNEP-WCMC, 2023), shade tree expansion represents a compelling, multi-benefit adaptation pathway, simultaneously delivering thermal buffering, carbon sequestration, and yield co-benefits (Keeble et al., 2024; Asitoakor et al., 2024).

5.4 Integrated Interpretation: Land Use, Vegetation Health, and Thermal Stress

The three analytical objectives converge on a mutually reinforcing narrative of coupled land-use and climate-driven cocoa system decline. Urbanisation and deforestation have simultaneously reduced productive cocoa area, degraded the thermal buffering capacity of the surrounding landscape, and directly elevated surface temperatures in remaining cocoa zones. The consequence declining NDVI and cocoa yield reflects the compound effects of these interacting stressors. Effective adaptation in Sunyani West will require concurrent action on forest conservation, agroforestry expansion, urban heat island mitigation, and protective land-use zoning, addressing both on-farm and off-farm factors that influence the thermal environment (Mensah et al., 2024).

6. Conclusions

This study presents the first 30-year longitudinal remote sensing assessment of cocoa land use, vegetation health, and land surface temperature dynamics in the Sunyani West Municipality, Ghana. The principal findings are:

(1) Closed-forest cover declined by 66% (from 26,937 ha to 9,046 ha) between 1994 and 2024, while built-up and bareland areas expanded by 89%, reflecting intense and sustained urbanisation pressure on the agricultural landscape.

(2) Mean NDVI within cocoa farm boundaries declined progressively from 0.72 in 1994 to 0.53 in 2024, indicating a substantial and sustained deterioration in cocoa vegetation health at the landscape scale.

(3) The extent of the municipality experiencing land surface temperatures exceeding 37°C increased six-fold from 2.37% in 1994 to 15.88% in 2024 amplified by urban heat island dynamics associated with built-up area expansion.

(4) A consistent inverse relationship was observed between LST and NDVI in cocoa zones, with yield minima (0.55–0.60 tons ha^{-1}) occurring in years of peak thermal anomaly, supporting the interpretation that landscape-scale thermal stress is a principal driver of declining cocoa productivity.

(5) Shade-tree cover functioned as a natural thermal buffer, with dense-canopy zones maintaining significantly lower LST and higher NDVI than exposed or degraded areas.

These findings carry direct practical implications: land-use planning frameworks must explicitly designate and protect agricultural land from urban encroachment; agroforestry promotion particularly shade tree expansion represents an evidence-based, multi-benefit adaptation strategy; and spatially targeted extension services should prioritise the identified stressed vegetation zones. At the methodological level, future studies should integrate red-edge vegetation indices and Sentinel-1 SAR data to complement NDVI analysis and improve cocoa canopy discrimination. The integration of remote sensing with ground-truth yield validation remains a priority for strengthening the predictive capability of satellite-based cocoa monitoring frameworks across West Africa.

Declarations

Funding

This research received no specific funding from public, commercial, or not-for-profit funding agencies.

Conflict of Interest

The author declares no conflict of interest.

Data Availability

Landsat imagery is freely available from the USGS Earth Explorer portal (https://earthexplorer.usgs.gov). Cocoa yield data are available from the Quality Control Division of COCOBOD upon request. Derived spatial datasets are available from the corresponding author upon reasonable request.

Ethics Approval

This study did not involve human participants, animal experiments, or sensitive data. No ethics approval was required.

Author Contributions

Prince Kwaku Mensah: Conceptualisation, data acquisition, formal analysis, methodology, writing — original draft, writing — review and editing.

Adiza Morro: writing — review and editing.

Henry Tei Apochie: Conceptualisation, writing — original draft, writing — review and editing.

References

1. Abdulai, I., Jassogne, L., Graefe, S., Asare, R., Van Asten, P., Läderach, P., & Vaast, P. (2018). Characterization of cocoa production, income diversification and shade tree management along a climate gradient in Ghana. PLoS ONE, 13(4), e0195777.
2. Acheampong, E. N., Bosu, P. P., & Opuni-Frimpong, E. (2021). Detection of stress areas in cocoa farms using GIS and remote sensing: A case study of Offinso Municipal & Offinso North district, Ghana. Scientific African, 13, e00664.
3. Agyei, T., Agyemang, M., Boateng, L. K., Addo, I. Y., & Asante, W. A. (2023). Understanding and addressing climate change impacts on cocoa farming in Ghana. Regional Sustainability, 4(4), 451–464.
4. Anim-Kwapong, G. J., & Frimpong, E. B. (2005). Vulnerability and adaptation assessment under NCCSAP2. Cocoa Research Institute of Ghana.
5. Anim-Kwapong, G. J., & Frimpong, E. B. (2006). Vulnerability of agriculture to climate change: Impact of climate change on cocoa production. Cocoa Research Institute of Ghana.
6. Asante, F. A., & Amuakwa-Mensah, F. (2015). Climate change and variability in Ghana: Stocktaking. Climate, 3(1), 78–99.
7. Asante, P., Rozendaal, D., Anten, N., Boeckx, P., Ewusi-Mensah, N., & Asare, R. (2025). Climate change impacts on cocoa production in the major producing countries of West and Central Africa by mid-century. Agricultural and Forest Meteorology, 360, 110263.
8. Asante, W. A., Acheampong, E., Kyereh, E., & Kyereh, B. (2017). Farmers' perspectives on climate change manifestations in smallholder cocoa farms in the forest-savannah transitional zone of Ghana. Land Use Policy, 66, 374–381.
9. Asare, R., Markussen, B., Asare, R. A., Anim-Kwapong, G., & Ræbild, A. (2017). On-farm cocoa yields increase with canopy cover of shade trees in two agro-ecological zones in Ghana. Climate and Development, 9(1), 17–29.

10. Ashiagbor, G., Asante, W. A., Forkuo, E. K., Acheampong, E., & Foli, E. (2022). Monitoring cocoa-driven deforestation in Ghana. Land Use Policy, 120, 106279.
11. Asigbaase, M., Dawoe, E., Sjogersten, S., & Lomax, B. H. (2021). The effectiveness of cocoa agroforests depends on shade-tree canopy height. Agriculture, Ecosystems & Environment, 322, 107647.
12. Asitoakor, B. K., Ræbild, A., Ravn, H. P., Eziah, V. Y., Owusu, K., Mensah, E. O., Vaast, P., & Asare, R. (2024). Impact of common shade tree species on microclimate and cocoa growth in agroforestry systems in Ghana. Agroforestry Systems, 98, 2027–2041.
13. Asner, G. P. (2001). Cloud cover in Landsat observations of the Brazilian Amazon. International Journal of Remote Sensing, 22(18), 3855–3862.
14. Babin, R., ten Hoopen, G. M., Cilas, C., Enjalric, F., Yede, Gidoin, C., & Lumaret, J. P. (2010). Impact of shade on the spatial distribution of Sahlbergella singularis in traditional cocoa agroforests. Agricultural and Forest Entomology, 12(1), 69–79.
15. Bempah, D. F., Asaaga, F., Ayamga, M., & Dinye, R. D. (2023). Peri-urbanisation and loss of arable land: Farmland access challenges and adaptation in Kumasi and Wa, Ghana. Land Use Policy, 124, 106449.
16. Chavez, P. S. (1988). An improved dark-object subtraction technique for atmospheric scattering correction of multispectral data. Remote Sensing of Environment, 24(3), 459–479.
17. Congalton, R. G., & Green, K. (2019). Assessing the Accuracy of Remotely Sensed Data: Principles and Practices (3rd ed.). CRC Press.
18. Forkuor, G., Dimobe, K., Serme, I., & Tondoh, J. E. (2022). Landsat-8 vs. Sentinel-2: Examining the added value of Sentinel-2's red-edge bands to land-use and land-cover mapping. GIScience & Remote Sensing, 55, 331–354.
19. Guthmann, A., et al. (2021). Evaluation of saturation behaviour in Sentinel-2 vegetation indices across high-biomass tropical systems. Spatial Information Research, 29(3), 371–384.
20. International Cocoa Organization. (2021). Quarterly Bulletin of Cocoa Statistics, Vol. XLVII, No. 4.
21. Jones, H. G., Serraj, R., Loveys, B. R., Xiong, L., Wheaton, A., & Price, A. H. (2009). Thermal infrared imaging of crop canopies for remote diagnosis of water stress. Functional Plant Biology, 36(11), 978–989.
22. Kabila, A., Adanu, S. K., & Agyemang, S. (2021). Urban expansion and agricultural land use change in Ghana. International Journal of Urban Sustainable Development, 13(2), 275–293.
23. Kalischek, N., Lang, N., Renier, C., Tondoh, J. E., Hiernaux, P., Baudron, F., & Wegner, J. D. (2023). Cocoa plantations are associated with deforestation in Côte d'Ivoire and Ghana. Nature Food, 4, 384–393.
24. Keeble, R., Rahman, S. A., Herbohn, J., Mahmood, H., Pienaar, E., & Darr, D. (2024). Low-emissions and profitable cocoa through moderate-shade agroforestry: Insights from Ghana. Agriculture, Ecosystems & Environment, 363, 108876.

25. Koranteng, A., Zawila-Niedzwiecki, T., Adu-Bredu, S., Nsiah Obeng, F., & Okdelegbah, P. (2020). Deforestation and landscape structural changes in Ghana's cocoa belt. Forests, 11(12), 1387.
26. Läderach, P., Martinez-Valle, A., Schroth, G., & Castro, N. (2013). Predicting the future climatic suitability for cocoa farming of the world's leading producer countries. Climatic Change, 119(3–4), 841–854.
27. Landis, J. R., & Koch, G. G. (1977). The measurement of observer agreement for categorical data. Biometrics, 33(1), 159–174.
28. Maes, W. H., & Steppe, K. (2019). Perspectives for remote sensing with unmanned aerial vehicles in precision agriculture. Trends in Plant Science, 24(2), 152–164.
29. Mensah, E. O., Vaast, P., Asare, R., Amoatey, C. A., Owusu, K., Asitoakor, B. K., Ræbild, A., & Ravn, H. P. (Eds.). (2024). Agroforestry as Climate Change Adaptation: The Case of Cocoa Farming in Ghana. Springer.
30. Moraiti, C., Hein, L., & Rosales, J. (2024). Evaluating Sentinel-2 red-edge indices for distinguishing cocoa agroforests from forest and mixed tree crops in West Africa. International Journal of Applied Earth Observation and Geoinformation, 125, 103609.
31. Ofori, A. B., Asante, J. N., Asubonteng, K. O., Mensah, F. O., Aboagye, L. M., Ehiakpor, K., Marfo, K. A., & Quainoo, A. K. (2022). Climate change manifestations and adaptations in cocoa farms: Perspectives of smallholder farmers in Adansi South District, Ghana. Heliyon, 8(11), e11515.
32. Osumanu, I. K., Aniah, P., & Yelfaanibe, A. (2020). Urbanization, agricultural land use change and livelihood adaptation strategies in peri-urban Wa, Ghana. SN Social Sciences, 1, 17.
33. Renier, C., Waldner, F., Jacques, D. C., Babah Ebbe, M. A., Callo-Concha, D., Rabe, J., Seguya, H., Tondoh, J. E., & Defourny, P. (2025). Direct and indirect deforestation for cocoa in the tropical moist forests of Ghana. Environmental Research Letters. https://doi.org/10.1088/2976-601X/add01b
34. Rouse, J. W., Haas, R. H., Schell, J. A., & Deering, D. W. (1974). Monitoring vegetation systems in the Great Plains with ERTS. Third ERTS Symposium, Vol. 1, pp. 309–317.
35. Ruf, F., Schroth, G., & Doffangui, K. (2015). Climate change, cocoa migrations and deforestation in West Africa. Sustainability Science, 10(1), 101–111.
36. Schroth, G., Läderach, P., Martinez-Valle, A., Bunn, C., & Jassogne, L. (2016). Vulnerability to climate change of cocoa in West Africa. Science of the Total Environment, 556, 231–241.
37. Sobrino, J. A., Jiménez-Muñoz, J. C., & Paolini, L. (2004). Land surface temperature retrieval from LANDSAT TM 5. Remote Sensing of Environment, 90(4), 434–440.
38. Tucker, C. J. (1979). Red and photographic infrared linear combinations for monitoring vegetation. Remote Sensing of Environment, 8(2), 127–150.
39. UNEP-WCMC. (2023). Mapping the potential for cocoa agroforestry in Ghana for climate change adaptation and mitigation. UNEP-WCMC, Cambridge, UK.
40. Vaast, P., & Somarriba, E. (2014). Trade-offs between crop intensification and ecosystem services: The role of agroforestry in cocoa cultivation. Agroforestry Systems, 88(6), 947–956.

41. Wessel, M., & Quist-Wessel, P. M. F. (2015). Cocoa production in West Africa, a review and analysis of recent developments. NJAS - Wageningen Journal of Life Sciences, 74–75, 1–7.
42. Wood, G. A. R., & Lass, R. A. (2008). Cocoa (4th ed.). Wiley-Blackwell.
43. Xue, J., & Su, B. (2017). Significant remote sensing vegetation indices: A review of developments and applications. Journal of Sensors, 2017, 1353691.
44. Zhu, Z., & Woodcock, C. E. (2012). Object-based cloud and cloud shadow detection in Landsat imagery. Remote Sensing of Environment, 118, 83–94.

Figures

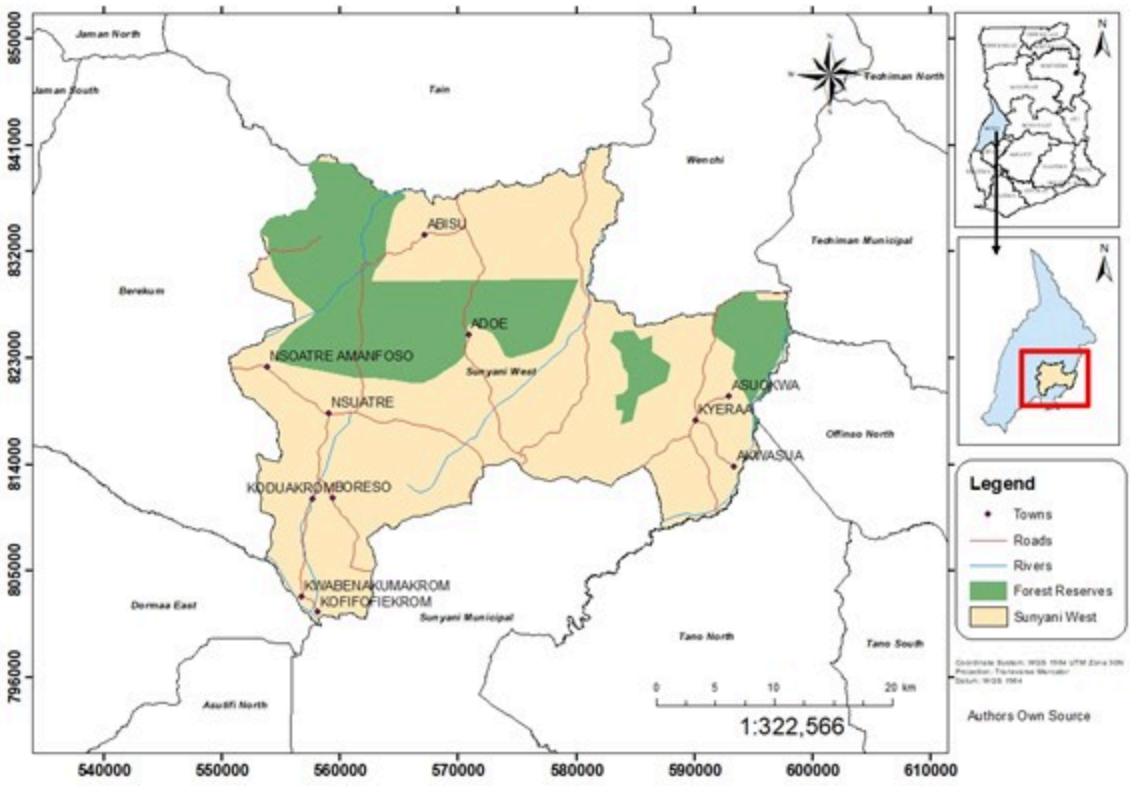


Figure 1

Location and administrative map of the Sunyani West Municipality, Bono Region, Ghana, showing major towns, roads, rivers, and forest reserve boundaries. Coordinate system: WGS 1984 UTM Zone 30N. Source: Authors' own compilation.

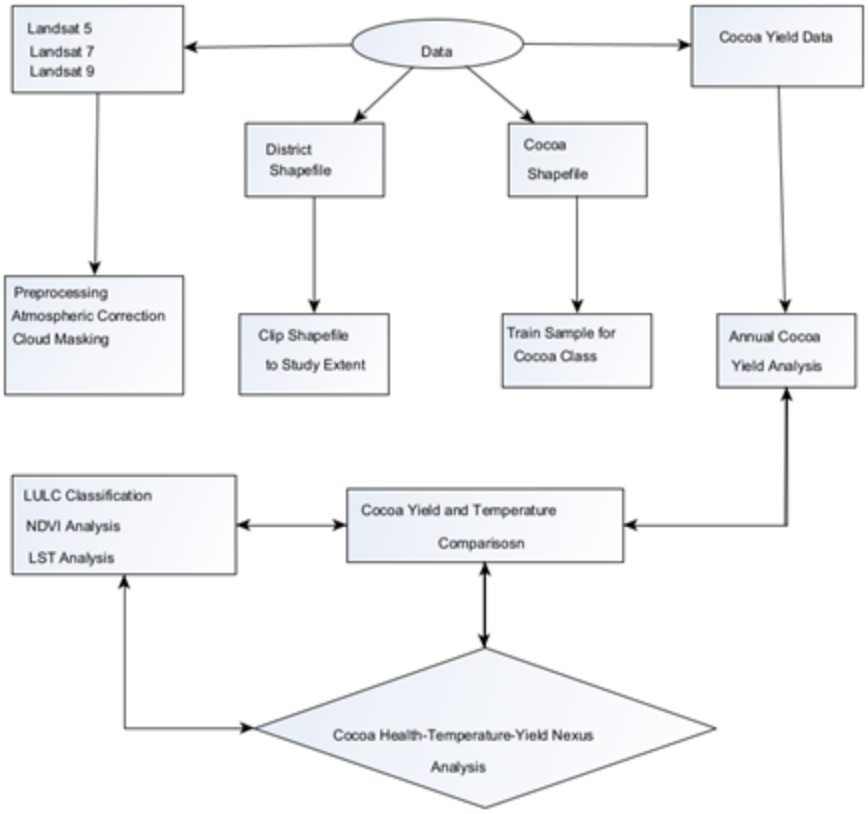


Figure 2

Methodological workflow illustrating data inputs, pre-processing steps, analytical procedures, and integration of remote sensing outputs with cocoa yield data.

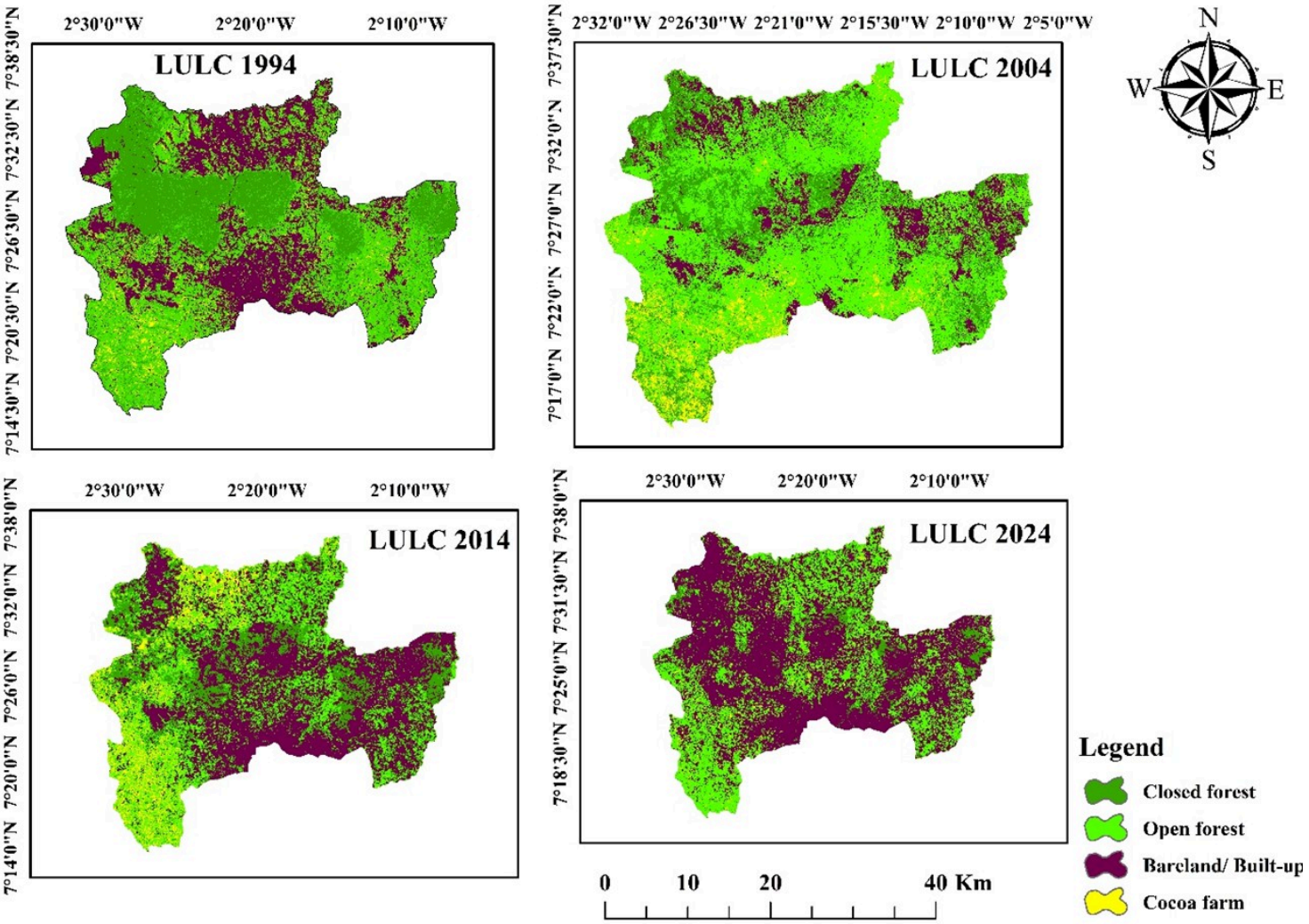


Figure 3

Land use/land cover classification maps of Sunyani West Municipality for 1994, 2004, 2014, and 2024 derived from Landsat imagery using Support Vector Machine classification.

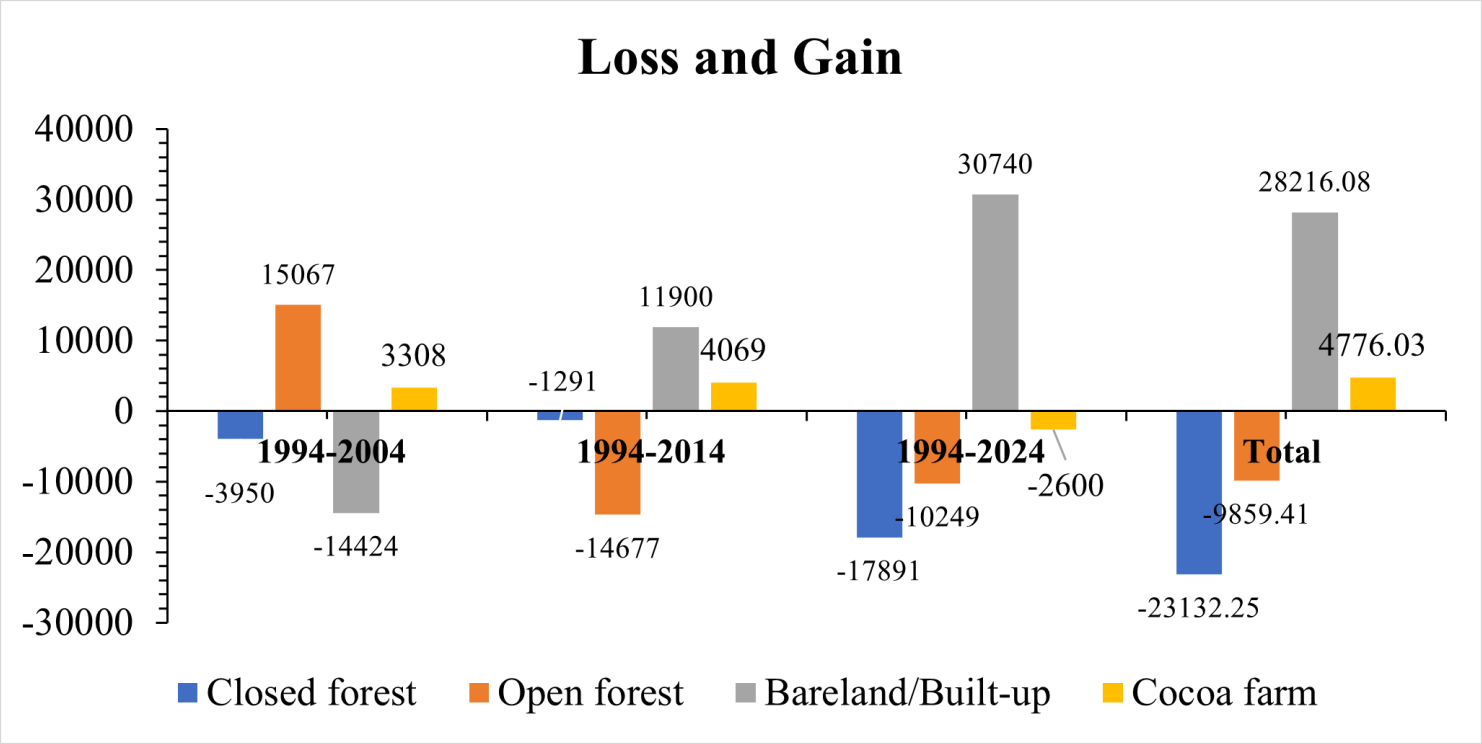


Figure 4

Figure 3: Graph showing LULC features Gain and Loss

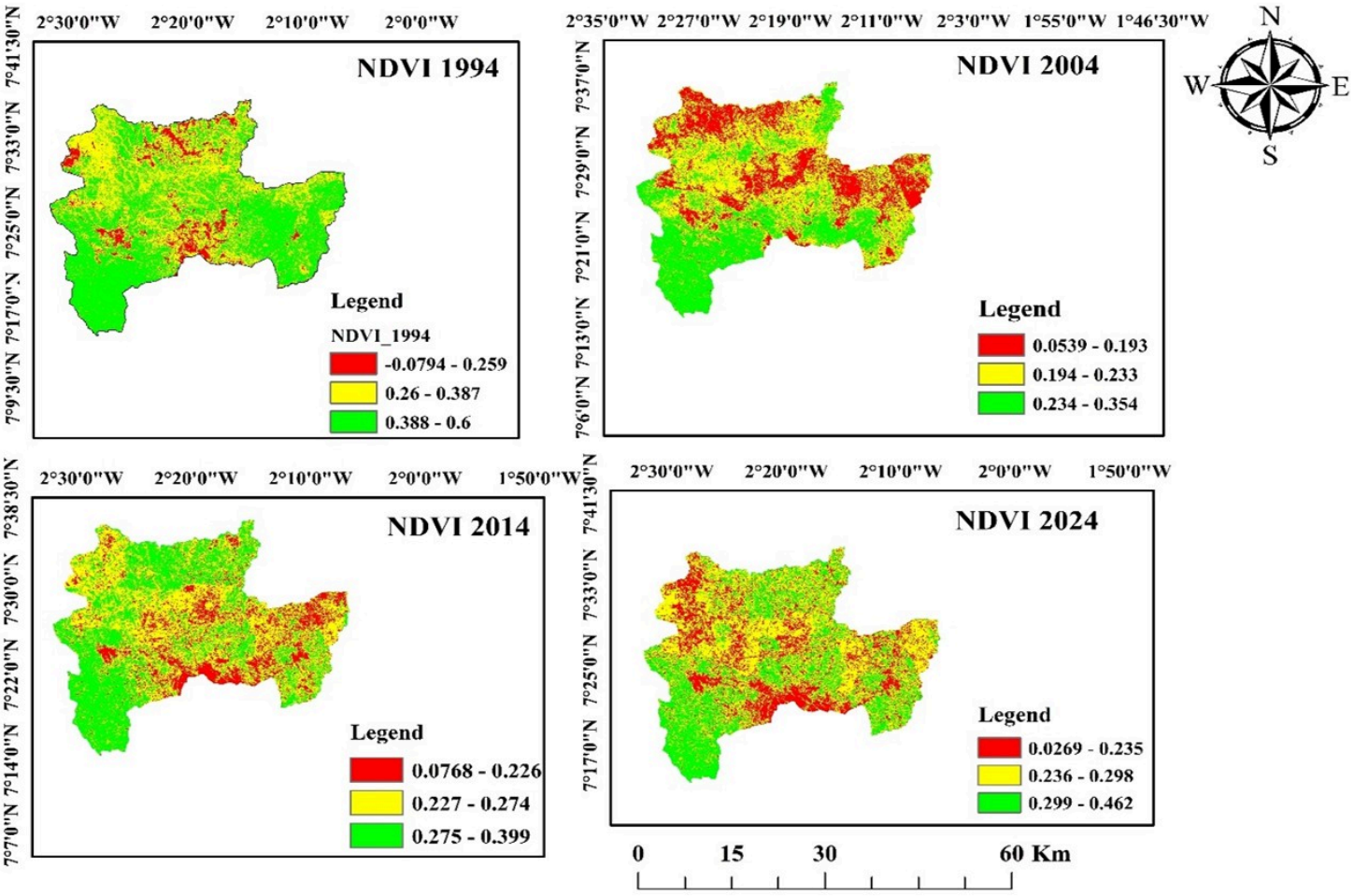


Figure 5

Fig. 4 Temporal NDVI maps of Sunyani West Municipality for 1994, 2004, 2014, and 2024. Green tones represent healthy vegetation (high NDVI); yellow and red tones indicate reduced photosynthetic activity and vegetation stress. The progressive decline in green coverage across epochs reflects deteriorating cocoa canopy condition.

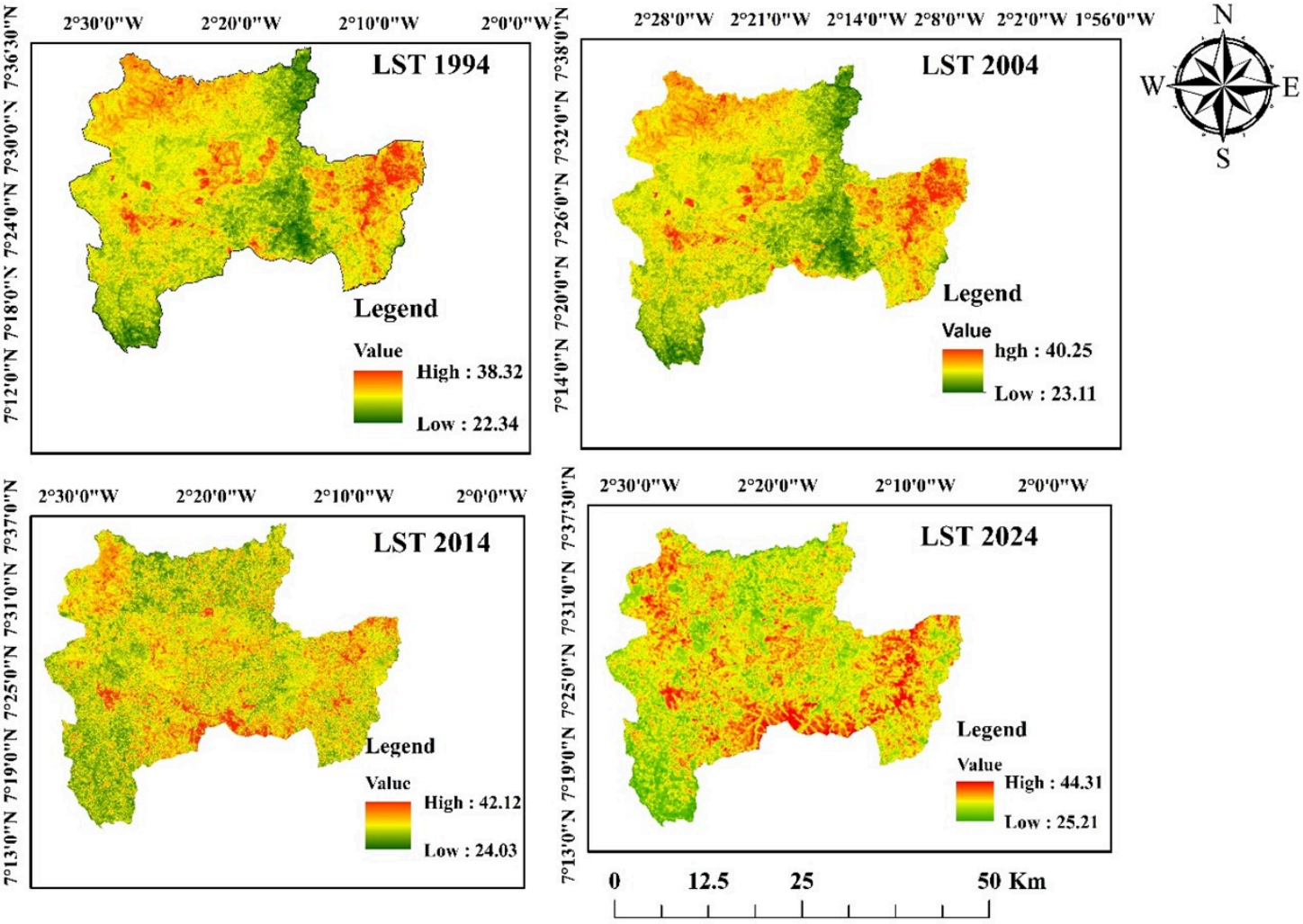


Figure 6

Fig. 5 Land surface temperature (LST) maps of Sunyani West Municipality for 1994, 2004, 2014, and 2024. The green-to-red colour ramp represents increasing surface temperature. Maximum LST increased from 38.32°C (1994) to 44.31°C (2024), with the most intense thermal anomalies concentrated in built-up and deforested areas.

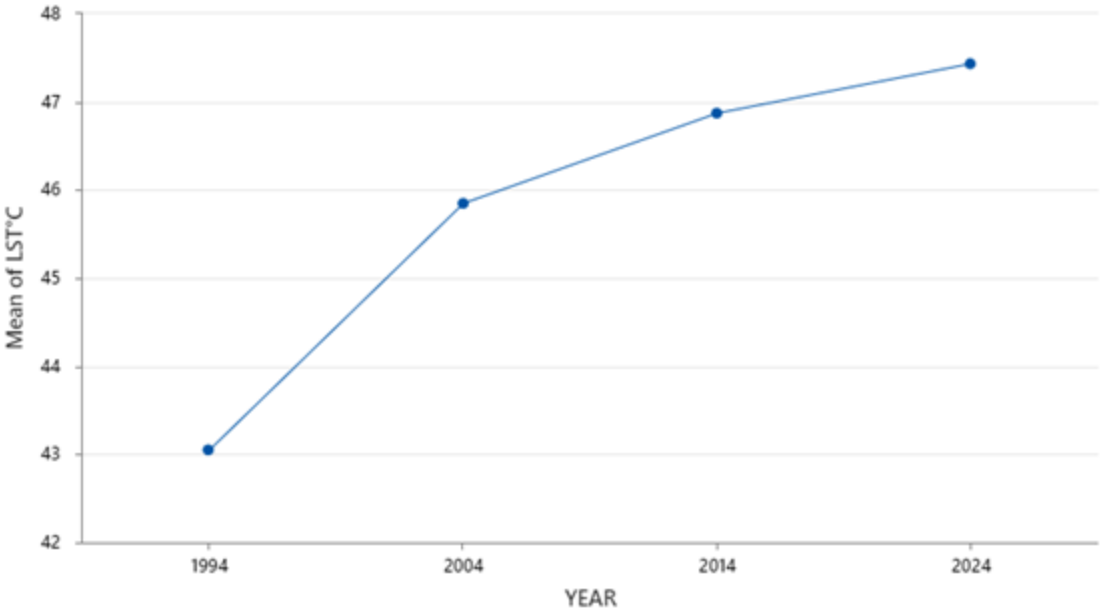


Figure 7

Fig. 6 Temporal trend in mean land surface temperature (°C) within the Sunyani West Municipality for the epochs 1994, 2004, 2014, and 2024, showing a sustained increase from approximately 43.1°C to 47.4°C over the 30-year study period.

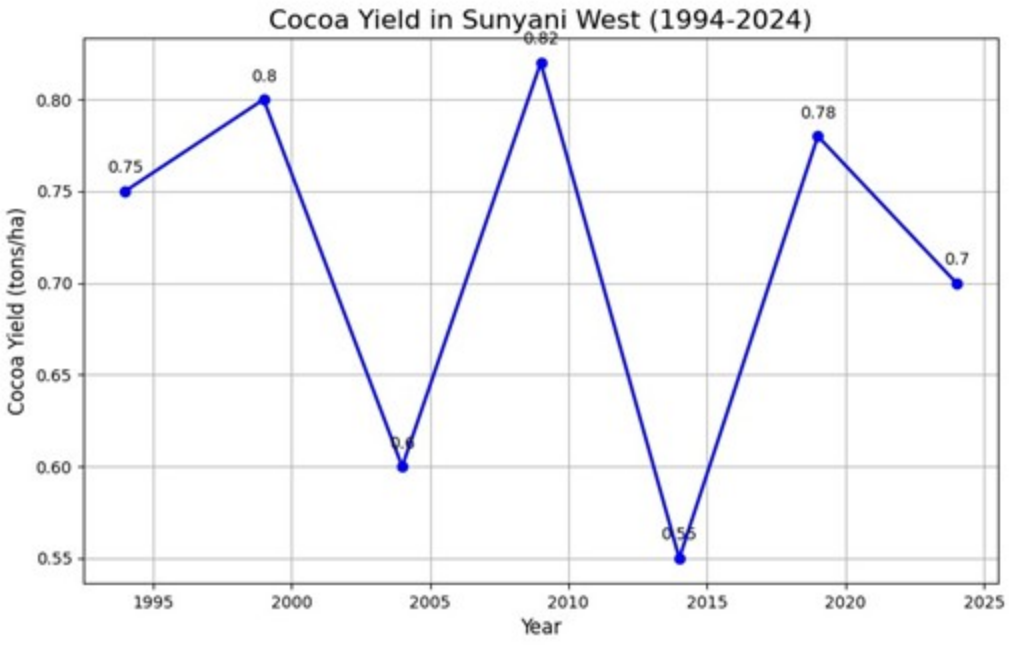


Figure 8

Fig. 7 Temporal trend in cocoa yield (tons ha⁻¹) in Sunyani West Municipality (1994–2024). Yield minima coincide with epochs of peak thermal anomaly (2004 and 2014), while relative recovery in 2010 and 2019 aligns with years of more favourable rainfall and lower thermal stress.